HARRAN ÜNİVERSİTESİ MÜHENDİSLİK DERGİSİ

HARRAN UNIVERSITY JOURNAL of ENGINEERING

e-ISSN: 2528-8733 (ONLINE)

CFD Analysis of the Impact of Temperature Variation on Condensation and Phase Transition Performance in Heat Exchangers

Isı Eşanjörlerinde Sıcaklık Değişiminin Yoğuşma ve Faz Geçiş Performansı Üzerindeki Etkisinin CFD Analizi

Yazar(lar) (Author(s)): *Fuat TAN[1], Hamid Orhun TUR[2]*

[1] ORCID ID: 0000-0002-4194-5591
[2] ORCID ID: 0009-0005-7850-6372

Bu makaleye şu şekilde atıfta bulunabilirsiniz (To cite to this article): Tan F., Tur H.O., "CFD Analysis of the Impact of Temperature Variation on Condensation and Phase Transition Performance in Heat Exchangers", ***Harran University Journal of Engineering***, 10(2): 80-93, (2025).

DOI: 10.46578/humder.1646589

HRU Muh Der, 10(2): 80-93 (2025)

Harran Üniversitesi Mühendislik Dergisi

Harran University Journal of Engineering

https://dergipark.org.tr/tr/pub/humder

Araştırma Makalesi

CFD Analysis of the Impact of Temperature Variation on Condensation and Phase Transition Performance in Heat Exchangers

Fuat TAN[1*], Hamid Orhun TUR[2]

[1,2]*Makine Mühendisliği Bölümü, Mühendislik Fakültesi, Balıkesir Üniversitesi, Balıkesir,Türkiye*

Article Information

Received: 17/02/2025
Revised: 07/04/2025
Accepted: 17/04/2025
Published: 30/06/2025

Tan F., Tur H.O., "CFD Analysis of the Impact of Temperature Variation on Condensation and Phase Transition Performance in Heat Exchangers", Harran University Journal of Engineering, 10(2): 80-93, (2025).

Abstract

This study investigates condensation in a rectangular copper heat exchanger with six circular tubes exposed to temperature variations. Three different temperature levels (380 K, 420 K and 460 K) were compared by examining heat transfer and phase change over a 5 second period with 1.25 s increments. A transient two dimensional analysis model was developed. Physical modeling was performed using the Volume of Fluid (VOF) phase model and the Standard k-ε turbulence model. The analysis results were monitored along two horizontal lines at different heights on the plate. The simulation results show that rapid condensation occurs at low and medium temperature levels due to high heat transfer. At the high temperature level, a delayed phase change leads to a longer condensation duration. The study serves as a guide for thermal device design by emphasizing the need to select appropriate temperature ranges while considering both the amount and duration of condensation.

Keywords: *CFD, Phase Transition, Heat Exchanger, Temperature, Condensation*

Isı Eşanjörlerinde Sıcaklık Değişiminin Yoğuşma ve Faz Geçiş Performansı Üzerindeki Etkisinin CFD Analizi

Makale Bilgisi

Başvuru: 17/02/2025
Düzeltme: 07/04/2025
Kabul: 17/04/2025
Yayınlanma: 30/06/2025

Tan F., Tur H.O., "Isı Eşanjörlerinde Sıcaklık Değişiminin Yoğuşma ve Faz Geçiş Performansı Üzerindeki Etkisinin CFD Analizi", Harran Üniversitesi Mühendislik Dergisi, 10(2): 80-93, (2025).

Öz

Yürütülen bu çalışma, sıcaklık değişimine maruz 6 adet dairesel boru içeren dikdörtgen bir bakır ısı eşanjöründeki yoğuşma konusunu incelemektedir. Üç farklı sıcaklık seviyesi (380 K, 420 K ve 460 K) ve 1,25 s artımlarla 5 saniye boyunca gerçekleşen ısı transferi ve faz geçişi ortaya konularak karşılaştırılmıştır. Geçici rejimde 2 boyutlu bir analiz modeli oluşturularak VOF (Volume of Fluid) faz modeli ve Standart k-ε türbülans modeli ile fiziksel modelleme yapılmıştır. Analiz sonuçları plaka üzerinde oluşturulan farklı yüksekliklerdeki yatay iki çizgi boyunca grafikle izlenmiştir. Simülasyon sonuçlarına göre, düşük ve orta sıcaklık seviyesinde yüksek bir ısı transferi neticesinde yoğuşma işleminin hızlıca gerçekleştiği gözlemlenirken, yüksek sıcaklık seviyesinde faz değişiminin gecikerek yoğuşma süresinin diğer sıcaklık seviyelerine göre arttığı gözlenmiştir. Çalışma, ısıl cihaz tasarımı yapılırken uygun sıcaklık aralıkları seçilerek yoğuşma miktarı ve süresinin de gözönünde bulundurulmasını ortaya koyan rehber niteliğinde bir çalışmadır.

Anahtar Kelimeler: *CFD, Faz Değişimi, Isı Eşanjörü, Sıcaklık, Yoğuşma*

*Corresponding author, e-mail: fuattan@balikesir.edu.tr
DOI: 10.46578/humder.1646589

1. INTRODUCTION (GİRİŞ)

In recent years, global energy consumption has increased. Inefficient energy conversions and higher fossil fuel use have caused major global issues [1]. To tackle this, two-phase closed thermosyphons have become popular. These systems efficiently transfer heat between surfaces and are widely used in renewable heating [2]. Grover introduced the concept of two-phase heat pipes in 1964 [3]. Two-phase thermosyphon systems show various operating conditions. Chen et al. [4]. studied these conditions and the influencing factors in detail. Several methods have been developed to solve multiphase computational fluid dynamics (CFD) problems. Common methods are Volume of Fluid (VOF) [5-6], front-tracking (FT) [7] and level-set (LS) [8-9]. VOF is widely used today in multiphase flow calculations. It tracks sharp interfaces, uses computational resources efficiently and is suitable for multiphase flows. Despite lower interface stability compared to other methods, VOF remains one of the most popular solutions [10-12].

Mroue et al. [13] conducted an experimental and numerical study of a heat pipe-based heat exchanger. Experimental data were compared with CFD simulations, where the heat pipe was modeled as solid rods with constant conductivity, showing agreement within 10%. In the simulations, the heat pipe was treated as a simple solid rod since two phase flow was not considered significant. In the study by Temimy et al. [14] a CFD simulation of a vertical heat pipe was analyzed using the VOF model. The effects of different charge ratios (40%, 50%, 60%, 70% and 100%) on the system were investigated, revealing interactions between rising hot vapor and condensed liquid. The results showed that the high momentum vapor phase pushes other phases away from the wall, increasing the efficiency of the heat pipe.

Lin et al. [15] developed a comprehensive 3D CFD model to simulate evaporation and condensation processes in a wickless heat pipe. The model used UDF and VOF methods, considering phase change materials during evaporation and condensation. The results were visualized using commercial software and validated experimentally with a transparent geyser. Song et al. [16] experimentally studied the thermal efficiency of a concentric annular heat pipe heat sink (CAHPHS). CAHPHS, made up of two circular tubes with different diameters, creates a vacuum vapor area, improving heat transfer and offering a more effective cooling solution than conventional heat pipes. The experiments tested various fill ratios, flow arrangements and heat values using different liquids like water and methanol. Results showed the best thermal performance with a 10% fill ratio for water and a 40% fill ratio for methanol. Yuan et al. [17] proposed a new dual-shell intermediary structure (called DSMHCTHE) to improve the heat transfer performance on the shell side by helically coiling test tubes. The performance of DSMHCTHE has been obtained by comparing the conventional multi-layer helically coiled tubes heat exchangers (MHCTHE) with the numerical results and experimental tests. The results showed that the proposed design is better in heat transfer even with the pressure loss on the shell side and it is 12% more comprehensive than MHCTHE in terms of total performance.

In their research, Li et al. [18] developed a model that considers the fin area of a compact heat exchanger to be the annular porous medium. They also proposed the computational fluid dynamics (CFD) numerical simulation method for a 3D dimpled tube heat exchanger with a flow layout simplified only by the dummy tube area. Their method enables the capturing of the flow characteristics in other areas by having a fine mesh only in the area where the flow occurs. Jin et al. [19] made a CFD model in the ANSYS Fluent program that can recover the waste heat by means of the electric generators and furnaces that emit the gaseous mixture with the water steam. Apart from generators and furnaces, the composition of the gaseous mixture occurs during the burning of certain fuels such as oil derived diesel. The invention of the mini heat exchangers allowed for increased heat transfer and the reduction of the heat exchanger's size.

In studies involving vapor-liquid phase change, the process is often simplified and defined as heat and mass transfer. Therefore, the phase change model used to describe heat and mass transfer is crucial for the accuracy and stability of CFD analysis. The most commonly used phase change model in CFD analysis of heat pipes is the Lee model, formulated by Lee, which assumes constant saturation pressure [20]. The Lee model was developed based on a set of Hertz-Knudsen equations derived from the kinetic energy theorem of gases. One advantage is that it allows phase change to occur both within phases and on surfaces and it can be easily applied to commercial CFD software using UDF [21]. Zhang et al. [22] have created a new phase transition model based on the Lee model to reduce numerical fluctuations in concentration simulations. By transferring energy sources to the adjacent grid points, the computational efficiency of the model was increased by a factor of 40. While the error rates for interface temperature and position with the developed model were only approximately 1%, the Lee model had an error of over 50%. Additionally, the use of R134a has been accomplished to analyze the Nusselt film condensation and forced convective condensation successfully resulting in a considerable improvement in accuracy compared to the previous numerical methods.

This study is a numerical analysis model that employs a computational fluid dynamics method to examine the condensation duration and amount in a six-tube heat exchanger at three different temperature levels. The research aims to use CFD to numerically interact with the effects of temperature variations on phase transition dynamics and condensation behavior in a rectangular copper heat exchanger. In the study, molecular dynamics simulations aided by VOF and Lee phase change models are performed to understand the dynamic behavior of the heat exchanger. The investigation runs the condensation at different thermal boundary conditions leading to the fabrication of a more rapid thermal management solution through the optimal choice of operating temperature.

2. MATERIAL AND METHOD

2.1. Material

One well-known equation for estimating net mass transfer between vapor and liquid surfaces during evaporation is the Hertz-Knudsen equation [23], shown below:

$$m = \alpha_c \frac{\sqrt{M}}{\sqrt{2\pi R}} \left[\frac{p}{\sqrt{T_v}} - \frac{p_{sat(T_1)}}{\sqrt{T_l}} \right] \tag{1}$$

In this equation, α_c is the accommodation coefficient. M is the molecular weight; R is the universal gas constant and P represents pressure. The result is expressed in kg/m²s. The Schrage and Lee models, often used for phase change in condensation and evaporation, are derived from this equation. Later, equation (1) was revised as follows.

$$m = \alpha_c \frac{\sqrt{M}}{\sqrt{2\pi RT}} [p - p_{sat}(T)] \tag{2}$$

According to the ideal gas law,

$$\rho = \frac{P_v M}{RT} \tag{3}$$

$$\frac{\sqrt{M}}{\sqrt{T}} = \frac{\sqrt{\rho R}}{\sqrt{p_v}} \tag{4}$$

By incorporating Equation (4) into Equation (2), Equation (5) is obtained as follows:

$$m = \frac{\alpha_c}{\sqrt{2\pi}} \sqrt{\rho_v} \frac{p - p_{sat(T)}}{\sqrt{p}} \tag{5}$$

CFD simulations use different methods to analyze mass transfer during phase changes. The mass transfer rate is added to the continuity equation through the source term S_m, representing mass change per unit volume. Equation (5) must be updated with the correct formula. The volumetric vapor-liquid interface area relates to the mean Sauter diameter D_{sm} and the phase volume fraction α [24]. The volumetric mass flow at the interfaces is expressed by the following formula:

$$m = \frac{6\alpha}{D_{sm}} \frac{\alpha c}{\sqrt{2\pi}} \sqrt{\rho_v} \frac{p - p_{sat}(T)}{\sqrt{p}} \tag{6}$$

In this system, α_c and D_{sm} change based on real conditions. The empirical coefficient β is defined as:

$$\beta = \frac{6\alpha_C}{D_{sm}\sqrt{2\pi}} \tag{7}$$

Substituting into Equation (6),

$$m = \beta\alpha\sqrt{\rho_v} \frac{p - p_{sat}(T)}{\sqrt{p}} \tag{8}$$

The mass transfer equations for liquid-to-vapor (evaporation) and vapor-to-liquid (condensation) transitions are obtained.

$$m_{I\to v} = \beta_e \alpha_I \sqrt{\rho_v} \frac{p_{sat}(T) - p}{\sqrt{p}} \tag{9}$$

$$m_{v\to l} = \beta_c \alpha_v \sqrt{\rho_v} \frac{p - p_{sat}(T)}{\sqrt{p}} \tag{10}$$

The empirical coefficients s^{-1}, β_e and β_c in Equations (9-10) should be determined under specific conditions for numerical accuracy. Interface tracking between phases is done by solving the mass conservation equation for volume fractions. The equation for the first phase is as follows:

$$\frac{1}{\rho_q}\left[\frac{\partial}{\partial t}(\alpha_q\rho_q) + \nabla\cdot(\alpha_q\rho_q\vec{v_q}) = \sum_{p=1}^{n}(\dot{m}_{pq} - \dot{m}_{qp})\right] \tag{11}$$

The VOF method is used to study two-phase flow and phase changes. In this study, liquid and vapor phases are used, so the total cell volume equals ($\alpha_v + \alpha_I = 1$). The continuity equation for the primary phase (liquid) is solved. Momentum and energy equations are calculated for the mixture phase. The equations are listed below.

The continuity equation is:

$$\frac{\partial}{\partial t}(\alpha\rho) + \nabla\cdot(\alpha\rho\mathbf{u}) = S_m \tag{12}$$

The momentum equation is:

$$\frac{\partial}{\partial t}(\rho u) + \nabla\cdot(\rho uu) = -\nabla p + \nabla\cdot[\mu(\nabla u + \nabla u^T)] + \rho g + S_{CSF} \tag{13}$$

In Equation (13), p represents local pressure, μ is dynamic viscosity and g denotes gravitational force. The energy equation is expressed as shown below [25].

$$\frac{\partial}{\partial t}(\rho E) + \nabla \cdot [(\rho E + p)u] = \nabla(k\nabla T) + S_E \tag{14}$$

In this equation, E represents internal energy and k denotes thermal conductivity.

In Equations (13-14), density ρ and viscosity μ are volume-averaged in the mixture phase. However, internal energy E is mass averaged.

Surface tension results from uneven molecular forces at liquid-vapor interfaces. It pulls molecules inward, aiming to minimize the energy of bubbles or droplets. This affects bubble formation and liquid adhesion to solid surfaces. The Continuum Surface Force (S_{CSF}) model accounts for these effects by adding a source term (S_{CSF}) to the momentum equation. This improves the accuracy of fluid dynamics modeling.

$$S_{CSF} = 2\sigma_{Iv}\frac{\alpha_I \rho_I C_v \nabla\alpha_v + \alpha_v \rho_v C_l \nabla\alpha_I}{\rho_I + \rho_v} \tag{15}$$

Eddy viscosity is used in turbulent flows to account for turbulence. It helps reduce errors and prevent micro-level fluctuations [26]. The general equation is:

$$v_t = C_\mu \frac{k^2}{\epsilon} \tag{16}$$

In the Eddy viscosity equation, v_t is Eddy viscosity (m²/s). C is the constant; k is turbulence energy and ϵ is energy dissipation.

2.2. Geometry

In this study, a 20x50 cm rectangular plate with six Ø7 mm copper tubes were used. Tube temperatures were examined at three levels (380K, 420K, 460K). The plate contained water vapor at 273K, and heat and vapor transfer were analyzed through the tube holes. Copper at the bottom condensed the vapor into liquid due to the high tube temperatures. 2D drawings and model image are shown in Figure 1.

In the analysis, water and vapor were the main fluids used for condensation and phase transition analysis in heat exchangers. Water was chosen to model vapor to liquid transition due to its high latent heat. The thermophysical properties of water and vapor are shown in Table 1.

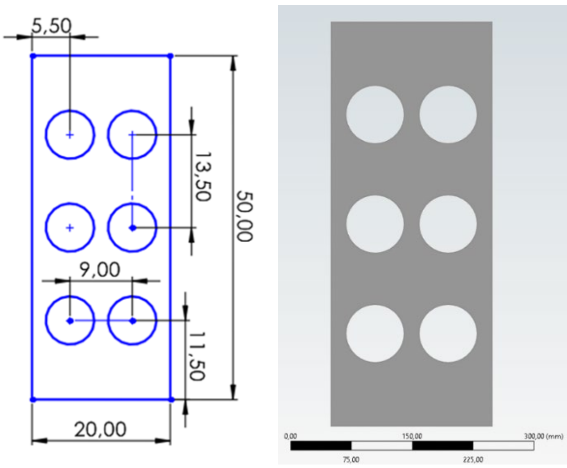

Figure 1. Model technical drawing (a) and image (b)

Table 1. Material properties

Property	Water-v	Water-l	Aluminum (Wall)
Density (ρ):	0.5542	998.2	2719
Specific heat (cp):	2014	4182	871
Thermal conductivity:	0.0261	0.6	202.4

2.3. Mesh

The geometry model uses mostly hexahedral elements, with tetrahedral elements around the tube holes, forming a hybrid mesh. The element size is 2.1 mm and the mesh was created with "Medium" smoothing. The mesh metrics are within recommended ranges. The model has 18,733 nodes and 18,107 elements. The mesh structure is shown in Figure 2 and the metrics are in Table 2.

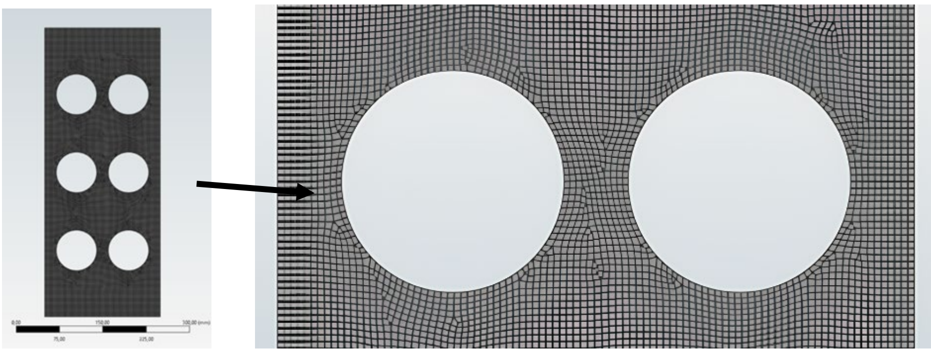

Figure 2. Mesh Structure

Table 2. Mesh metric values

Mesh Metric	Min	Max	Average
Aspect Ratio	1	2,4686	1,0608
Skewness	4,508e-7	0,59079	5,7044e-2
Orthogonal Quality	0,75212	1	0,99086

2.4. Boundary Conditions

CFD analyses were done using Ansys Fluent under steady state conditions. The ambient temperature was set to 273K, and the water-vapor phase volume fraction was defined as 1. The vapor fraction was applied using the patch method. The edge temperatures of six tubes, called "condenser1" were set to 380K, 420K and 460K. The lower edge of the plate, "condenser2" was set to 273K.

The standard k-ε turbulence model and Enhanced Wall Treatment were used for the analysis. The standard k-ε turbulence model served as the reliable method adopted in this research because of its exact prediction of separated flows in the recirculation zone and the boundary layer such as in the case of condensation dominated phase change. This model entails the solution of transport equations for turbulence kinetic energy (k) and its dissipation rate (ε), thus it is the best choice for high Reynolds number and low anisotropy flows. Moreover, it provides numerical stability. The VOF method is also handy in dealing with the tracking of both liquid and vapor interfaces during an unsteady simulation. According to Fadhl et al. [10], the standard k-ε model yields reliable results in two-phase thermosyphon systems with condensation, balancing computational cost and physical realism. The VOF model simulated the vapor to liquid phase transition. The surface tension between liquid and vapor was set to 0.06 N/m. Mass transfer occurred through condensation, so the evaporation-condensation model was used. The Lee model was applied for analysis.

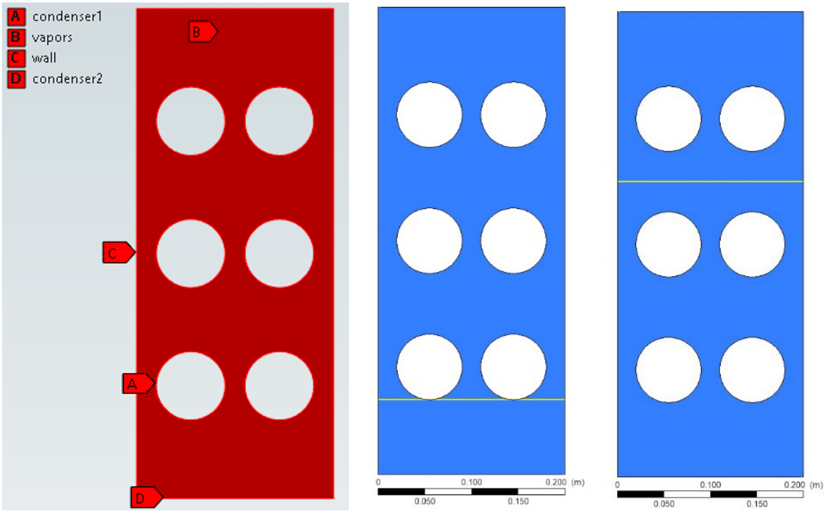

Figure 3. Boundary conditions

Table 3. Boundary conditions

Boundary	**1**	**2**	**3**
"Condenser1" Temp.	380 K	420 K	460 K
Turbulence Model	k-ε	k-ε	k-ε
Multiphase Model	VOF	VOF	VOF
Mass Transfer Model	Lee Model	Lee Model	Lee Model

3. RESULTS and DISCUSSIONS

The contour results show that water vapor distribution and temperature changes over time. Below are detailed interpretations for each temperature level. This study's CFD analyses examined condensation and phase transitions at 380K, 420K and 460K. At 380K, condensation starts much faster. Over time (t=1.25 - 5 s), water vapor decreases quickly as molecules transition to liquid. Due to the lower energy level, condensation takes place quicker than at other temperatures which gives rise to rapid condensation from vapor and a swift change of phase.

380 K results:

At 380K, temperature distribution is uniform across the surface. Over time (t=1.25-5 s), temperature differences decrease quickly. The lower temperature allows for faster phase transition and quicker thermal equilibrium. This indicates that condensation at 380K is more efficient and takes less time.

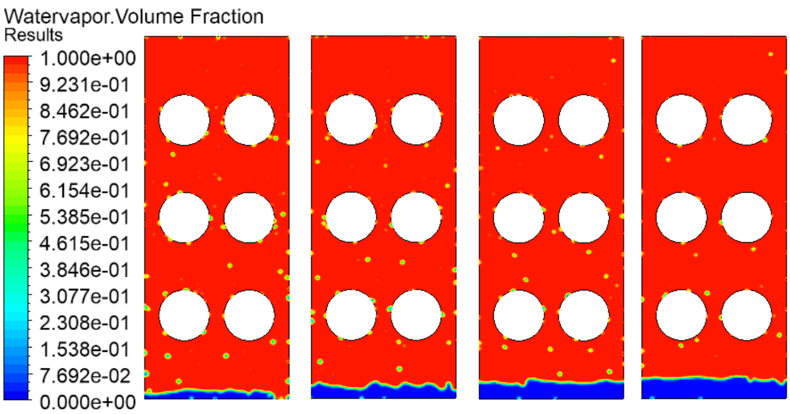

Figure 4. Water vapor distribution for 380 K **a)** t= 1.25 s **b)** t=2.5 s **c)** t=3.75 s **d)** t= 5 s

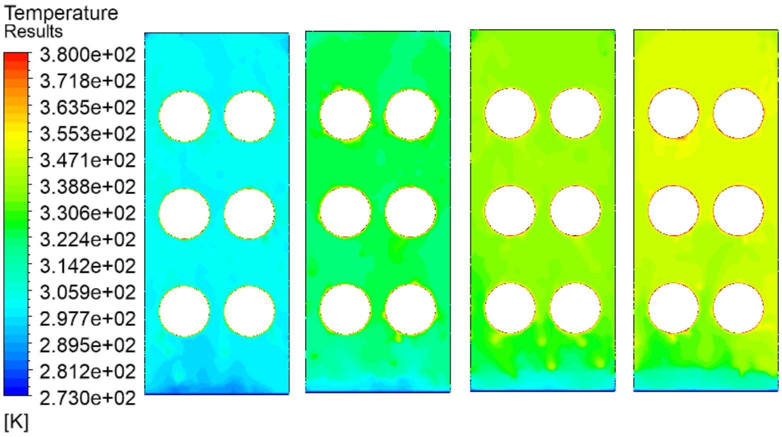

Figure 5. Temperature distribution for 380 K **a)** t= 1.25 s **b)** t=2.5 s **c)** t=3.75 s **d)** t= 5 s

420 K results:

Steam condenses on the pipes and loses energy. The high energy delays the process. At 420K, condensation is slow and gradual. Over time, water vapor decreases but condensation still takes longer than at 380K.

At 420K, the temperature gradually decreases, with noticeable cooling around the tubes. Temperature changes are slower than at 380K and surface differences are more pronounced. As time progresses (t=1.25-5 s), the system nears thermal equilibrium but temperature differences last longer due to the higher heat.

At 460K, temperature differences are more pronounced. Surface temperature changes vary widely and cooling is much slower. Condensation is delayed and thermal equilibrium takes longer. Even as the system cools (t=1.25-5 s), slow condensation keeps the differences significant.

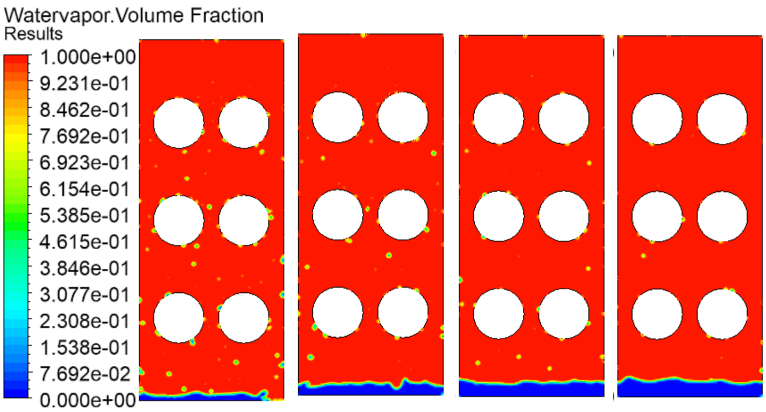

Figure 6. Water vapor distribution for 420 K **a)** t= 1.25 s **b)** t=2.5 s **c)** t=3.75 s **d)** t= 5 s

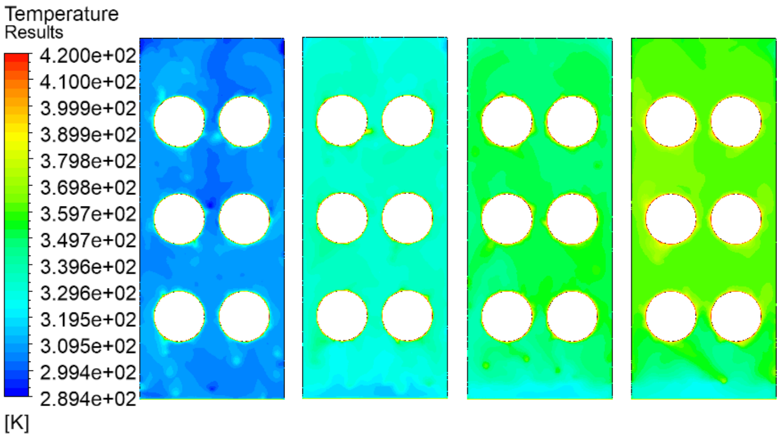

Figure 7. Temperature distribution for 420 K **a)** t= 1.25 s **b)** t=2.5 s **c)** t=3.75 s **d)** t= 5 s

460 K results:

The process where vapor molecules change to liquid whilst giving off dissipates energy is referred to as condensation. This is much slower as it depends on the created thermal energy in addition to the pressure.

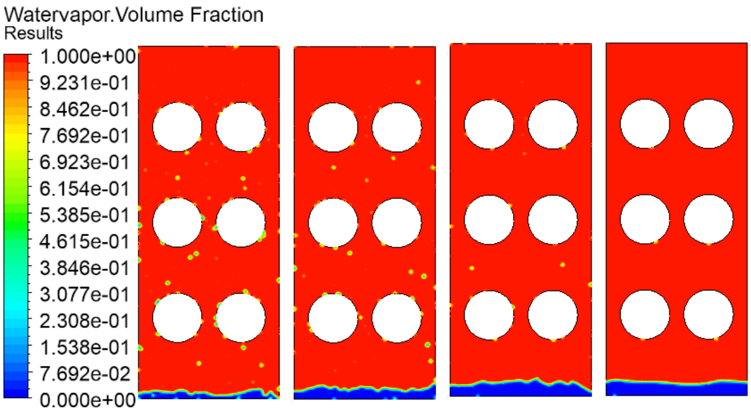

Figure 8. Water vapor distribution for 460 K **a)** t= 1.25 s **b)** t=2.5 s **c)** t=3.75 s **d)** t= 5 s

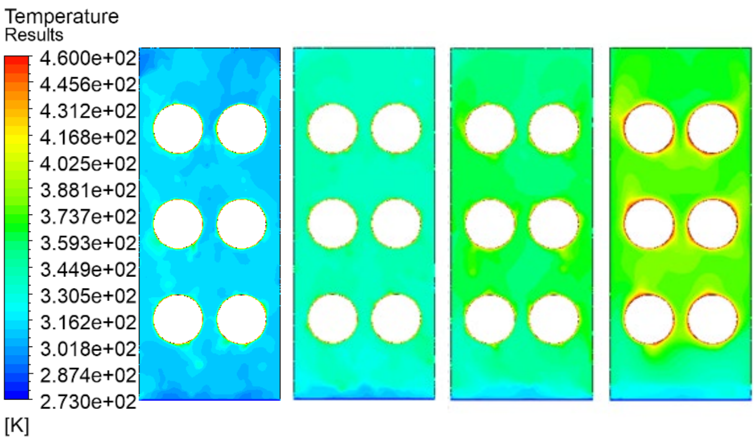

Figure 9. Temperature distribution for 460 K **a)** t= 1.25 s **b)** t=2.5 s **c)** t=3.75 s **d)** t= 5 s

At higher temperature, vapor molecules possess more energy while needing to condense which takes even more energy. The increased temperature further retards the condensation process.

Figure 10. Temperature distribution at line 2

The changes of the variable x on the graph in terms of temperature suggest that the condensation process is effective over the surface. Each detached section from the base line reaches the same thermal reading which suggests that every section of the surface goes through the same process. It indicates the high ratio of effectiveness of the process of phase change. The temperature differences were large at 460K. Only notable t = 1.25s did temperatures span between 312.6K to 364.6K. While at 5s the range had increased to 372K to 440K. Due to the lack of energy in the system, the rate of condensation was reduced, which explained a wide range of temperature readings over the surface. The transition of phase was slower due to an increase in molecular energy and so did the rate of energy supply to the system.

At 420K, temperature distribution was more stable but still varied. At t = 1.25 s, temperatures ranged from 309.5 K to 333.7 K. At t = 5 s, they varied between 351.4 K and 380.5 K. Condensation was slower than at 380K and temperature differences persisted longer. This indicates that the condensation process took more time and delayed energy loss in the vapor phase. At t = 1.25 s, temperatures ranged from 296.1 K to 315.7 K. By t = 5 s, they dropped to 347.4 K to 351.8 K. Lower energy in water vapor facilitated rapid condensation and reduced temperature differences quickly. A significant amount of heat energy was released during phase transition, allowing swift thermal equilibrium.

Figure 11. Temperature distribution at line 1

At 460K, temperature differences were observed over the widest range. At T = 1.25 s, the upper limit and the lower limit of the temperature range were 311.7 K and 316.2 K respectively. At t = 5 s, the range of the temperatures was from 352.8 K to 440.0 K. The condensation process at this high temperature proceeded at a very slow rate. This resulted in large temperature gradients along the surface. Phase change was completed later because the energy of molecules was high. Energy transfer took place over a longer time span.

At 420K, the heat distribution got balanced more slowly than it balanced in 380K. At t = 1.25 s, temperatures varied between 308.3 K and 308.1 K. At t = 5 s, the temperature range was wider, and it was from 357.7 K to 380.5 K. The slower condensation process resulted in longer lasting temperature differences. Even at t = 5 s, the differences in temperature persisted and were wider than at other levels. This indicates that condensation was more sluggish and energy dissipation in the gas phase was postponed.

At 380K, the distribution of the temperature range over time became uniform. At t = 1.25 s, temperature ranged from 301.2 K to 303.8 K while the variation at t = 5 s in temperature range was drastically lower from 347.4 K to 349.5 K. The lower energy of vapor caused a fast condensation process. This led to a quick reduction in temperature differences along the surface. A significant amount of heat energy was transferred out during the phase transition, allowing the system to reach thermal equilibrium quickly.

4. CONCLUSION

This study explores condensation and phase transition phenomena in heat exchanger systems featuring circular tubes placed on a rectangular plate. Some analysis at 380K, 420K and 460K showed that temperature variation directly influences the what is the condensation rate, transition phase effectiveness and the system integrated performance. These results inform the profound influence of temperature changes on heat transfer. As a result, the study revealed several key findings about the temperature of the phase transition and condensation:

- At the temperature level of 380K, the analysis showed that the condensation process started quickly and completed in a short time. At lower temperatures, water vapor molecules have lower energy. This leads to faster energy loss needed for the phase transition. As a result, the system reached the thermal equilibrium more rapidly and temperature differences decreased quickly. The fast condensation process also enabled more efficient heat transfer.

- At 420K, the condensation process was more gradual and lasted longer than at 380K. Temperature differences along the surface were maintained for an extended period. The phase transition slowed but showed more stability. This may benefit applications that aim to optimize temperature distribution, as condensation occurred more evenly.

- At 460K, the phase transition process was the slowest. Condensation started late and temperature differences were broader. High temperature delayed energy loss in vapor phase molecules. This extended the phase change duration and reduced system efficiency. The slow condensation caused delays in heat transfer, which is undesirable for energy efficiency.

The present study's results are in agreement with previous numerical and experimental findings as reported in the literature. The rapid condensation and heat transfer at lower temperatures shown in this study are similar to the findings of Temimy et al. [14] who have reported the efficiency of condensation is increased under the condition of lower thermal loads. In addition, the delayed transition at the higher temperature is comparable to the results of Fadhl et al. [10] where the greater energy of the vapor resulted in longer condensation times. The correlation between these studies confirms that the thermal performance of two-phase systems is highly dependent on the initial temperature conditions, which has been demonstrated through the use of CFD based analyses in the heat exchanger investigations are cited in this report.The results show that temperature control is vital for improving heat exchanger efficiency. Efficient heat transfer occurs at lower temperatures. High temperatures slow down the condensation process. Therefore, optimized heat exchanger designs are recommended for various temperature scenarios

CONFLICT OF INTEREST

The authors declare that there is no conflict of interest between them.

STATEMENT OF PUBLICATION ETHICS

The authors of the paper submitted declare that nothing which is necessary for achieving the paper requires ethical committee and/or legal-special permissions.

AUTHOR STATEMENT

Fuat Tan: Analysis, investigation, writing, methodology.
Hamid Orhun Tur: Recources, writing, methodology.

REFERENCES

[1] W. Srimuang, W., Amatachaya, P. (2012). A review of the applications of heat pipe heat exchangers for heat recovery. Renewable and Sustainable Energy Reviews, 16(6), 4303-4315.

[2] Schneider, D., Lauer, M., Voigt, I., & Drossel, W. G. (2016). Development and examination of switchable heat pipes. Applied thermal engineering, 99, 857-865.

[3] Faghri, A. (2018). Heat pipes and thermosyphons. Handbook of thermal science and engineering, 2163-2211.

[4] Chen, X., Gao, P., Tan, S., Yu, Z., & Chen, C. (2018). An experimental investigation of flow boiling instability in a natural circulation loop. International Journal of Heat and Mass Transfer, 117, 1125-1134.

[5] Yankov, G. G., Milman, O. O., Minko, K. B., & Artemov, V. I. (2023). Simulation of the condensation processes of R113 in a horizontal pipe by the VOF method. Thermal Engineering, 70(11), 860-874.

[6] Su, Z., Li, Z., Wang, K., Kuang, Y., Wang, H., & Yang, J. (2024). Investigation of improved VOF method in CFD simulation of sodium heat pipes using a multi-zone modeling method. International Communications in Heat and Mass Transfer, 157, 107669.

[7] M Najafian, M., & Mortazavi, S. (2023). A numerical study of drop evaporation at high density ratios using Front-Tracking method. Computers & Mathematics with Applications, 134, 1-15.

[8] Tang, M., Xin, Z., & Wang, L. (2024). Physics-Informed neural network for level set method in vapor condensation. International Journal of Heat and Fluid Flow, 110, 109651.

[9] Lyras, P., Hubert, A., & Lyras, K. G. (2023). A conservative level set method for liquid-gas flows with application in liquid jet atomisation. Experimental and Computational Multiphase Flow, 5(1), 67-83.

[10] Fadhl, B., Wrobel, L. C., & Jouhara, H. (2015). CFD modelling of a two-phase closed thermosyphon charged with R134a and R404a. Applied Thermal Engineering, 78, 482-490.

[11] Yang, Z., Peng, X. F., & Ye, P. (2008). Numerical and experimental investigation of two-phase flow during boiling in a coiled tube. International Journal of Heat and Mass Transfer, 51(5-6), 1003-1016.

[12] Fadhl, B., Wrobel, L. C., & Jouhara, H. (2013). Numerical modelling of the temperature distribution in a two-phase closed thermosyphon. Applied Thermal Engineering, 60(1-2), 122-131.

[13] Mroue, H., Ramos, J. B., Wrobel, L. C., & Jouhara, H. (2015). Experimental and numerical investigation of an air-to-water heat pipe-based heat exchanger. Applied Thermal Engineering, 78, 339-350.

[14] Temimy, A. A., & Abdulrasool, A. A. (2019, May). CFD Modelling for flow and heat transfer in a closed Thermosyphon charged with water–A new observation for the two phase interaction. In IOP Conference Series: Materials Science and Engineering (Vol. 518, No. 3, p. 032053). IOP Publishing.

[15] Lin, Z., Wang, S., Shirakashi, R., & Zhang, L. W. (2013). Simulation of a miniature oscillating heat pipe in bottom heating mode using CFD with unsteady modeling. International Journal of Heat and Mass Transfer, 57(2), 642-656.

[16] Song, E. H., Lee, K. B., Rhi, S. H., & Kim, K. (2020). Thermal and flow characteristics in a concentric annular heat pipe heat sink. Energies, 13(20), 5282.

[17] Yuan, Y., Cao, J., Zhang, Z., Xiao, Z., & Wang, X. (2024). Experimental and numerical simulation study of a novel double shell-passes multi-layer helically coiled tubes heat exchanger. International Journal of Heat and Mass Transfer, 227, 125497.

[18] Z. Li, Z. Z., Ding, Y. D., Liao, Q., Cheng, M., & Zhu, X. (2021). An approach based on the porous media model for numerical simulation of 3D finned-tubes heat exchanger. International Journal of Heat and Mass Transfer, 173, 121226.

[19] Ebrahimnia-Bajestan, E., Gharibnavaz, M., Jin, M., Li, R., Brinkerhoff, J., & Milani, A. (2022). CFD Simulation of Condensation Heat Transfer In Mini/Micro-Channels—Application In Waste Heat Recovery.

[20] Lee, W. H. (1980). A pressure iteration scheme for two-phase flow modeling. Multiphase transport fundamentals, reactor safety, applications, 1, 407-431.

[21] Wang, X., Wang, Y., Chen, H., & Zhu, Y. (2018). A combined CFD/visualization investigation of heat transfer behaviors during geyser boiling in two-phase closed thermosyphon. International Journal of Heat and Mass Transfer, 121, 703-714.

[22] Zhang, Y., Li, G., Zhang, G., & Ding, S. (2023). Development and modified implementation of Lee model for condensation simulation. Applied Thermal Engineering, 231, 120872.

[23] Knudsen, M., (1934). The kinetic theory of gases, methuen & co. London Ltd, 1.
[24] De Schepper, S. C., Heynderickx, G. J., & Marin, G. B. (2009). Modeling the evaporation of a hydrocarbon feedstock in the convection section of a steam cracker. Computers & Chemical Engineering, 33(1), 122-132.
[25] Jouhara, H., Fadhl, B., & Wrobel, L. C. (2016). Three-dimensional CFD simulation of geyser boiling in a two-phase closed thermosyphon. International Journal of Hydrogen Energy, 41(37), 16463-16476.
[26] Prandtl, L. (1942). Bemerkungen zur Theorie der freien Turbulenz. ZAMM-Journal of Applied Mathematics and Mechanics/Zeitschrift für Angewandte Mathematik und Mechanik, 22(5), 241-243.